Autophagy

Taylor & Francis

! " # ! $" %%&&&' ( ) ! "'* $%! %+ ,

) ! " - * " ! - ") " - " -

. / 0 # 1 " 0 2" 3 0 / 0 4" / 0 3 / 0 #
5 " 4 0 # / 6 1 7 "

8 * " - Dan!L"i, Jing-Zfi-fi-

A fluorescent tool set for yeast Atg proteins

Dan Li,[1] Jing-Zhen Song,[2] Mei-Hua Shan,[2] Shi-Ping Li,[2] Wei Liu,[2] Hui Li,[1] Jing Zhu,[3] Yue Wang,[2] Jianping Lin,[2] and Zhiping Xie[1,*]

[1]School of Life Sciences and Biotechnology; Shanghai Jiao Tong University; Shanghai, China; [2]Nankai University; Tianjin, China; [3]School of Life Sciences; Tsinghua University; Beijing, China

Fluorescence microscopy of live cells is instrumental in deciphering the molecular details of autophagy. To facilitate the routine examination of yeast Atg proteins under diverse conditions, here we provide a comprehensive tool set, including (1) plasmids for the expression of GFP chimeras at endogenous levels for most Atg proteins, (2) RFP-Atg8 constructs with improved properties as a PAS marker, and (3) plasmids for the complementation of common yeast auxotrophic markers. We hope that the availability of this tool set will further accelerate yeast autophagy research.

Introduction

Autophagy is a well-conserved intracellular degradation pathway in eukaryotes.[1-4] By removing obsolete or damaged cytoplasmic components, autophagy serves to maintain cellular health, especially under stress conditions. A key step in the autophagy pathway is the formation of autophagosomes, which are double-membrane vesicles responsible for the sequestration and transport of degradation targets. Yeast genetic studies conducted 2 decades ago led to the identification of autophagy-related proteins.[5] To date, more than 30 Atg proteins have been discovered, many of which have homologs or functional analogs in multicellular organisms. Considering the young age of the field, it is not surprising that our understanding of the function of most Atg proteins remains primitive. It is safe to predict that in the foreseeable future, research on these existing and other still unidentified Atg proteins will continue to attract new scientists.

One simple yet powerful technique in cell biology research, including autophagy, is live cell fluorescent microscopy. By expressing fluorescent protein chimeras, the subcellular localization and trafficking of a protein can be monitored in vivo. Researchers using yeast *Saccharomyces cerevisiae*

color. The excitation and emission spectra of the fluorescent protein pair must differ enough to allow the clear separation of their respective signal. Both the CFP and YFP pair, and the GFP and RFP pair satisfy this requirement. The use of the CFP and YPF pair is handicapped by the low brightness and photostability of CFP.[10] Modern RFPs generally possess better properties.[11] Nevertheless, the use of RFP-tagged Atg proteins in yeast has been limited, possibly due to the poor signal or function of the chimeras.

To facilitate the routine examination of the subcellular localization of existing Atg proteins and the characterization of new players in autophagy, we set out to create a fluorescent tool set containing plasmids for the efficient tagging of most Atg protein with one or 2 copies of GFP and a bright and functional RFP-Atg8 construct for using as a PAS marker. We also constructed plasmids for the complementation of auxotrophic defects in commonly used yeast strains, which should help avoid potential complications in data interpretation.

Results

AtgX-GFP and 2xGFP set

Currently, there are more than 30 Atg proteins in *Saccharomyces cerevisiae* (note that Atg25, Atg28, Atg30, and Atg35 are only present in other yeast species). To reduce the workload, we omitted the following when constructing our toolset: (1) proteins specifically involved in mitophagy and pexophagy, (2) receptors for the Cvt complex, (3) cytosolic enzymes involved in the modification of Atg8 and Atg12, (3) Atg12, which requires N-terminal tagging,[12] (4) Atg15, a vacuolar lipase, and (5) Atg22, a vacuolar amino acid permease. We set out to construct plasmids for tagging of most of the remaining Atg proteins with GFP by a 2-step process. We first generated tagged strains using the traditional PCR-based approach. Using the genomic DNA of the strains as templates, we then cloned corresponding DNA fragments containing large homologous regions at both ends and inserted each into a Bluescript plasmid. In the case of GFP-Atg8, we designed a new plasmid with the goal of ensuring single copy integration into the *ura3* locus (**Fig. S1**). Hence we obtained a total of 19 plasmids for tagging of Atgs 1, 2, 5, 6, 8, 9, 11, 13, 14, 16, 17, 18, 20, 21, 23, 24, 27, 29, and 31 (**Table S1**). Based on our limited experience, the use of these plasmids resulted in greatly improved transformation efficiency over the PCR-based approach. More importantly, the targeting precision is much better. For most of the plasmids, generally more than 80% of the tranformants were correct.

All 19 chimeras produced detectable fluorescence signals (**Fig. S2, S3 and S4**). The chimeras of Atg1, Atg2, Atg5, Atg8, Atg11, Atg13, Atg14, Atg16, Atg17, Atg29, and Atg31 displayed the typical "PAS pattern," generally a perivacuolar punctum. The chimeras of Vps30/Atg6, Atg18, and Atg21 localized to multiple perivacuolar puncta plus the vacuolar rim. The chimeras of Atg9, Atg20, Atg23, Atg24, and Atg27 displayed multiple puncta, many of which were away from the vacuole. Some Atg27-GFP was present on the vacuolar membrane. This phenomenon appeared to be strain background-dependent, as it was absent in a BY4741-derived strain (data not shown). The signal intensity of the chimeras varied greatly among different Atg proteins. GFP-Atg8 was the brightest. The chimeras of Atg1, Atg2, Atg18, Atg20, Atg21, and Atg24 were in the next tier. The rest were further down the rank. To ease the detection of these less abundant Atg proteins, we then constructed a second plasmid set for tagging with 2 copies of GFP (**Table S1**). A template plasmid with 2 copies of GFP was engineered first. The chimeras were then obtained using the same 2-step approach as described above. Most 2xGFP chimeras retained the localization patterns of their 1xGFP counterparts (**Fig. S2, S3**), except for Atg16-2xGFP. Atg16-2xGFP displayed diffuse signal in the cytosol with no perivacuolar puncta (data not shown). We therefore omitted the Atg16-2xGFP construct in subsequent analysis.

We then tested the functionality of these constructs by the Pho8Δ60 assay and Ape1 maturation assay (**Fig. 1**).[13,14] The Pho8Δ60 assay measures the nonselective delivery of cytosolic material to the vacuole by autophagy. Most tagged proteins retained their functionality in this assay (**Fig. 1A**). Atg9 suffered the most from GFP-tagging, leading to approximately 50% drop in autophagic flux. The Ape1 maturation assay measures the selective transport of Cvt complex to the vacuole. Among existing Atg proteins, Atg11, Atg20, Atg21, Atg23, Atg24, and Atg27 are known to have a greater impact on the Cvt pathway than on nonselective autophagy.[1,2] All 12 tagged strains contained some levels of mature Ape1, indicating the chimeras are at least partially functional in the Cvt pathway (**Fig. 1B**).

Improved RFP-Atg8

When characterizing a new protein potentially involved in autophagosome formation, it is often informative to examine whether this protein is ever present at the PAS. Among all the known Atg proteins, the amount of Atg8 at the PAS is the highest, making it an ideal marker.[15] However, our experience with RFP-Atg8 variants used in the existing literature indicated that the signal of these chimeras is substantially weaker than that of GFP-Atg8, which is further compounded by their reduced photostability. Over the past few years, we have also constructed RFP-Atg8 variants based on mCherry and mKO.[10] Despite their good theoretical brightness, neither fared any better (**Fig. S5A** and data not shown). Furthermore, constructs based on mCherry have a tendency to accumulate in the vacuole (**Fig. S5A**), which interferes with the observation of perivacuolar structures.

In the search for a better RFP-Atg8 construct, we found that Atg8 fused to DsRed Express 2 (hereafter referred to as DRE) did not display the strong vacuolar signal typical of mCherry chimeras (**Fig. S5A**), although the brightness was slightly lower.[16] DRE processes good properties in photostability and maturation kinetics. We therefore chose to incorporate tandem copies of DRE to improve the signal. As DRE exists in oligomers, we designed linker peptides that would allow the intramolecular oligomerization of tandem DRE domains (**Fig. S6**). We estimated the length of the linkers from the crystal

structure of DRE. We then searched a linker database (http://www.ibi.vu.nl/programs/linkerdbwww/) and selected short and long peptides necessary for the construction of tandem dimer and tetramers (**Tables S2, S3**).[17] After modeling of the resulting structures by Modeler 9.10 and Amber 12,[18,19] we settled on one option for the short linker and 2 options for the long linker. We named the tandem dimer DuDre and the tetramers QuDre and QuDre 2, respectively.

We subsequently constructed the corresponding Atg8 chimeras and tested their functionality (**Fig. 1C**). DuDre-Atg8 led to good recovery of autophagy activity in *atg8*Δ cells only when moderately overexpressed by the *CUP1* promoter. A similar level of recovery was obtained with QuDre-Atg8 expressed by the *ATG8* promoter. But when overexpressed, QuDre-Atg8 produced no autophagy activity. QuDre 2-Atg8 did not perform well under the same conditions. In *atg8*Δ cells, both *CUP1*p-DuDre-Atg8 and *ATG8*p-QuDre-Atg8 displayed the perivacuolar punctate signal typical of GFP-Atg8 (**Fig. S6A and B**). A similar fluorescent signal pattern was observed for *CUP1*p-DuDre-Atg8 expressed in wild-type cells (**Fig. S7A**). However, *ATG8*p-QuDre-Atg8 produced fewer and dimmer puncta in wild-type cells (**Fig. S7B**), suggesting that endogenous Atg8 competes with QuDre-Atg8. Encouraged by the performance of DuDre-Atg8, we constructed another plasmid using tdTomato, which is also a tandem dimer variant of RFP. The functionality of tdTomato-Atg8 was close to that of DuDre-Atg8 (**Fig. 1C**), although the photostability was not as good (**Fig. S5C**).

As a demonstration of the efficacy of our new RFP-Atg8 constructs in labeling the PAS in dual-color imaging, we cotransformed yeast cells with *CUP1*p-DuDre-Atg8 and select GFP-tagging plas-

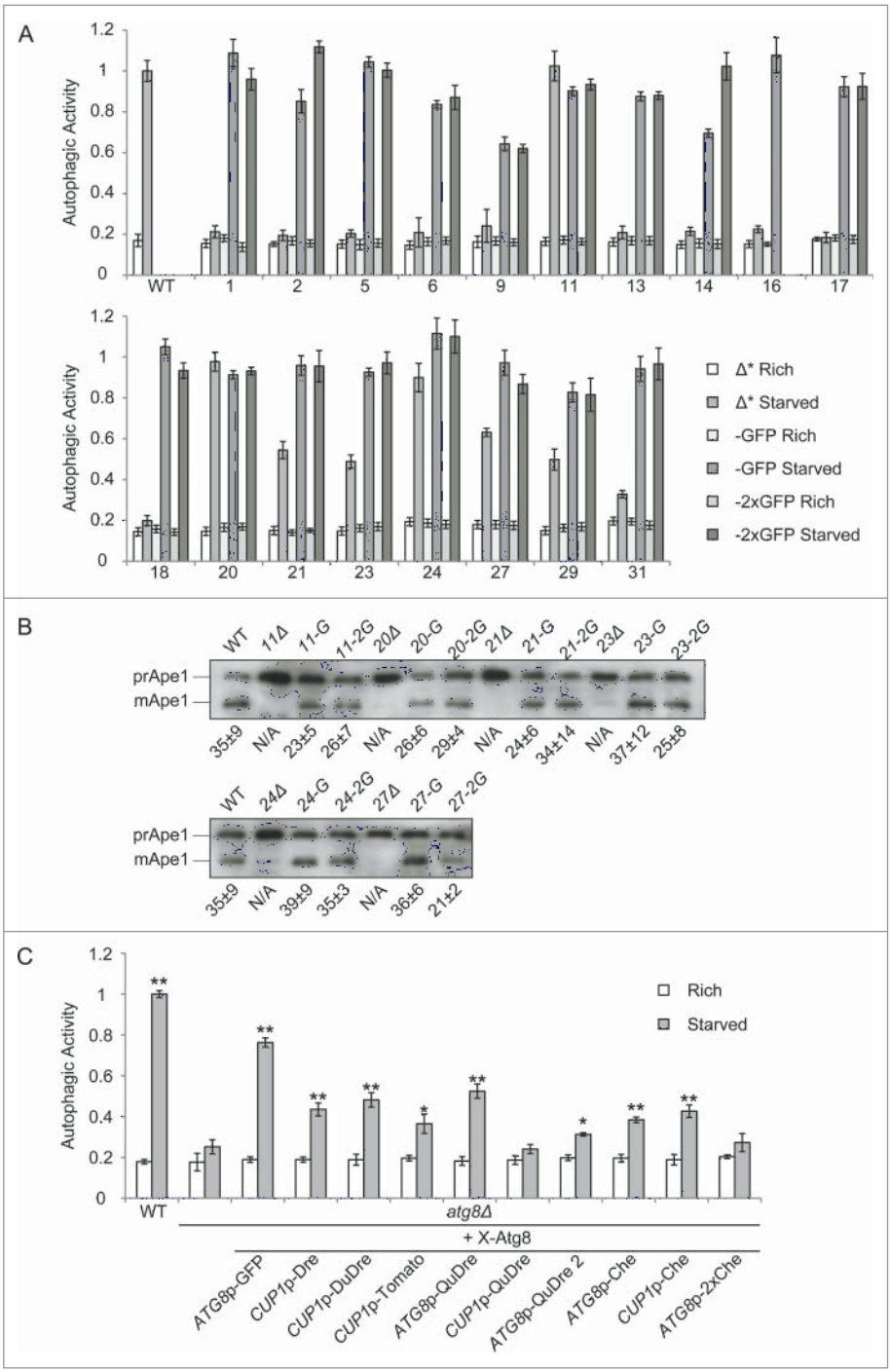

Figure 1. Functionality of GFP and RFP constructs. (**A**) Functionality of GFP and 2xGFP chimeras in nonselective autophagy. The autophagic activities of the indicated strains were measured by the Pho8Δ60 assay. As only *ATG* genes are concerned, "*ATG*" was omitted in the labels for simplicity. Δ*, *ATG* gene knockouts (*: except for the WT group). -GFP and -2xGFP: GFP and 2xGFP tagged strains for the indicated *ATG* gene. Rich: cells cultured in YPD medium. Starved, cells starved in SD-N medium for 4 h. Error bar, standard deviation, n = 3. (**B**) Functionality of GFP and 2xGFP chimeras in the Cvt pathway. Yeast cells with the indicated genotype were grown to mid-log phase in YPD medium. Protein samples were collected and analyzed by western blotting. prApe1, precursor Ape1. mApe1, mature Ape1. Numbers below the images: percentage of mature Ape1 (mean ± standard deviation, n = 4). N/A, not available. (**C**) Functionality of GFP and RFP-Atg8 chimeras. The autophagic activities of wild-type cells and *atg8*Δ cells expressing the indicated constructs were measured by the Pho8Δ60 assay. Rich: cells cultured in YPD medium. Starved, cells starved in SD-N medium for 4 h. Error bar, standard deviation, n = 4. T test was performed against *atg8*Δ samples (**, $P < 0.01$; *, $P < 0.05$).

mids representative of different functional groups of Atg proteins. Under starvation conditions, DuDre-Atg8 displayed clear colocalization with all the Atg proteins tested (**Fig. 2**). Among them, Vps30/Atg6 displayed the minimal rate of colocalization, possibly because the autophagy-specific phosphatidylinositol-3 kinase complex I only contains a minor fraction of total Vps30/Atg6.[20] In contrast, the rate of colocalization with Atg14, the subunit exclusive to complex I, was comparable with the rest. The localization patterns of most tested GFP chimeras were unaffected by coexpression of DuDre-Atg8, except for Atg1, Atg9, and Atg18 (**Fig. S8**). Puncta formation of both Atg1 and Atg18 was slightly reduced in the presence of DuDre-Atg8, which possibly explains the higher incidence of bright Atg9 puncta occurrence. Over all, these data indicate that *CUP1*p-DuDre-Atg8 can be used as a reliable PAS marker.

Auxotrophic marker set

Autophagy is closely connected with metabolism. In fact, the most widely used approach for inducing autophagy in yeast is nitrogen starvation. For historical reasons, common laboratory yeast strains generally contain auxotrophic mutations to facilitate further genetic manipulation.[21] The corresponding genes are mostly involved in the metabolism of amino acids and nucleotides. In our routine work, we have found that some of these genes have clear strain-dependent impacts on the regulation of autophagy, as measured by the Pho8Δ60 assay (**Fig. 3**). To avoid potential complications in data interpretation, we constructed a set of integration plasmids for the purpose of complementing any remaining auxotrophic defects once all desired manipulations are finished. Here we focused on 5 strains frequently used in autophagy research: BY4741, BY4742, SEY6210, TN121, and TN124.[14,21,22] Accordingly, we constructed 6 plasmids, covering *LEU2, LYS2, MET15, HIS3, TRP1*, and *URA3* (**Table S1**). As all are integration plasmids, once the transformants are obtained, all strains can be cultured with complete media, which helps standardize the testing conditions.

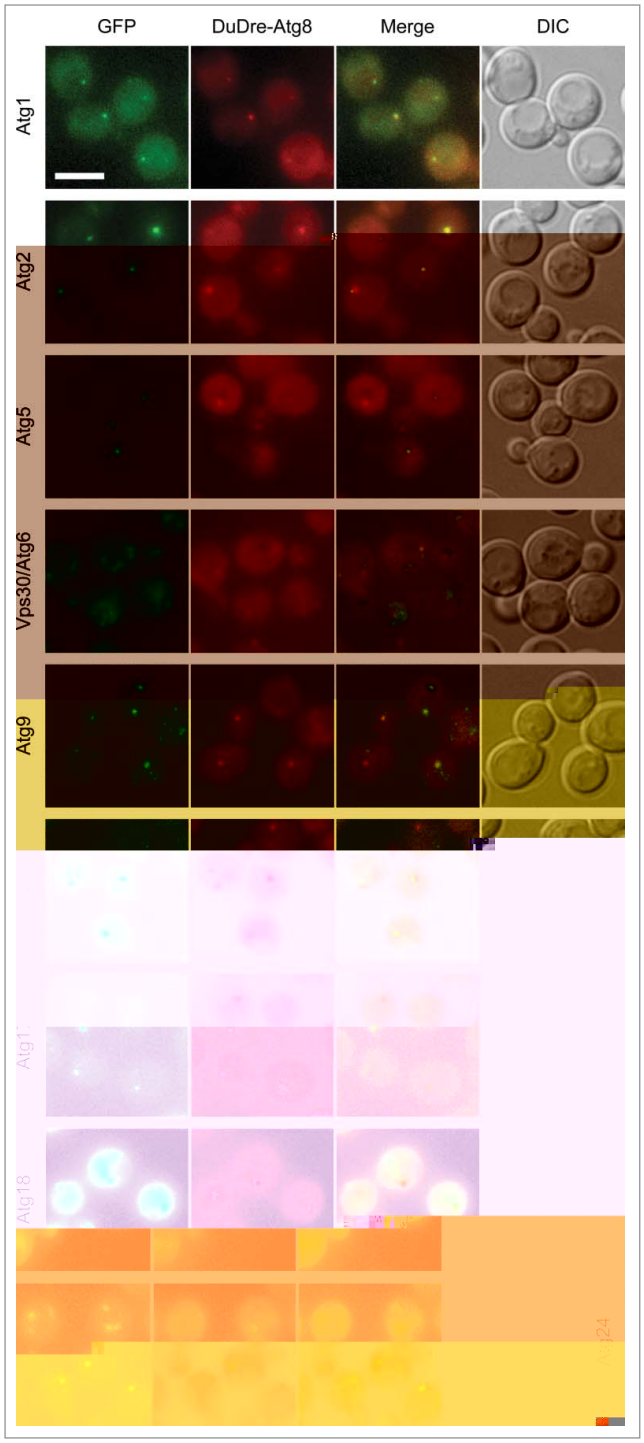

Figure 2. Colocalization of GFP-tagged Atg proteins with DuDre-Atg8. Wild-type yeast cells were cotransformed with *CUP1*p-DuDre-Atg8 and GFP or 2xGFP tagging plasmids for the indicated protein. Atg1 and Atg24 were tagged with GFP; the remaining were tagged with 2xGFP. Cells were starved in SD-N medium for 1 h before observation. The experiment was repeated 3 times. Representative projection images containing colocalized puncta are shown. Scale bar: 5 μm.

Discussion

In this study, we constructed a tool set containing the following groups of plasmids for yeast autophagy research: (1) plasmids for the tagging of 19 Atg proteins with one or 2 copies GFP, (2) plasmids for the expression of functional

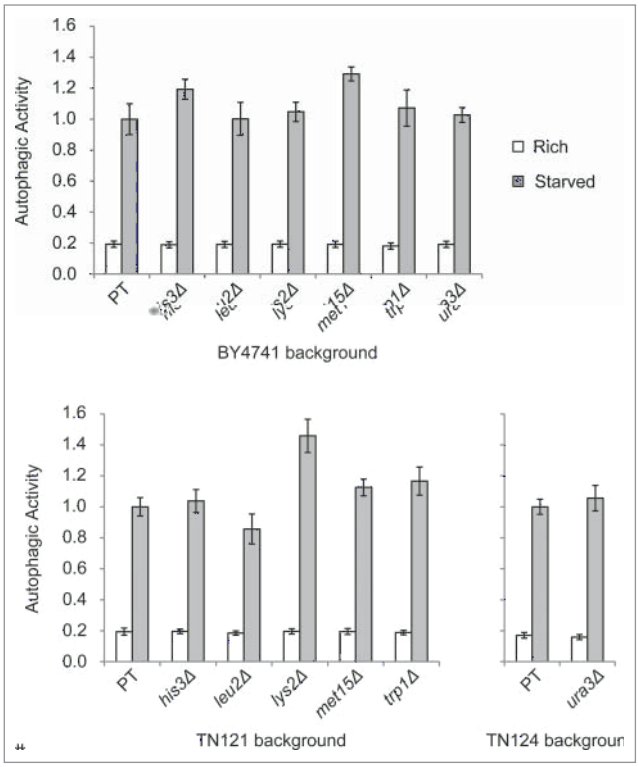

Figure 3. Impact of common auxotrophic markers on autophagy. *pho8Δ60 pho13Δ* strains derived from BY4741, TN121, or TN124 were converted to prototrophs (PT) or auxotrophs lacking one of the commonly used markers. The autophagic activities of the indicated strains were measured by the Pho8Δ60 assay. Rich: cells cultured in YPD medium. Starved, cells starved in SD-N medium for 4 h. Error bar, standard deviation, n = 4.

RFP-Atg8 variants as PAS markers, and (3) plasmids for the complementation of common auxotrophic defects. All plasmids were designed to be integrated into the genome.

The long homologous region in the GFP-tagging plasmids leads to high targeting precision. All GFP-tagging plasmids were designed to allow the integration of only one copy in haploid yeast. Provided that multiple biological repeats are examined, prior verification of transformants by PCR or western blotting can be skipped to speed up research progress when using these plasmids. In this aspect, the practical benefits of using our plasmid set are similar to those offered by an existing centromeric toolset constructed by Ma et al.[23] Their set is based on the Gateway cloning system, which allows easy swapping with other tags. It covered 14 YFP-tagged Atg proteins plus additional proteins in nonautophagy pathways. In contrast, our integration set is focused specifically on Atg proteins tagged with one or 2 copies of GFP. We chose integration-plasmid-based strategy for 2 reasons. The first is that genome integration avoids cell-to-cell variations in the copy numbers of carried constructs, which would otherwise translate into cell-to-cell variations in fluorescent signal intensity. The second is that once verified, the transformants can be cultured in complete media, such as YPD, which help simplify and standardize the experimental set up.

The continued development in fluorescent proteins offers great potential in simultaneous imaging of multiple proteins in live cells. However, the realization of this potential in yeast autophagy research has been hindered by the availability of functional and bright RFP chimeras. Our efforts produced 3 viable options for RFP-Atg8. *CUP1*p-DuDre-Atg8, *CUP1*p-tdTomato-Atg8 and *ATG8*p-QuDre-Atg8 all produce better signals than existing constructs. The choice between *CUP1*p-DuDre-Atg8 and *CUP1*p-tdTomato-Atg8 is straightforward, as the latter is limited by its photostablity. The situation between *CUP1*p-DuDre-Atg8 and *ATG8*p-QuDre-Atg8 is a bit more complicated. *ATG8*p-QuDre-Atg8 enjoys the advantage of being expressed by the endogenous *ATG8* promoter. The problem with *ATG8*p-QuDre-Atg8 is that if additional Atg8 protein is present, the competition renders QuDre-Atg8 less efficient at labeling the PAS. Thus for the purpose of labeling the PAS, we recommend the use of *CUP1*p-DuDre-Atg8 unless one takes the effort to knock out endogenous *ATG8*.

The intimate relationship between autophagy and metabolism is an important topic in autophagy research.[24] For researchers not specifically focused on this area, we recommend converting all the strains to be tested back to a prototrophic form once all the planned genetic manipulations are done. The new set of complementing plasmids should meet the needs of most researchers using strains derived from BY4741, BY4742, SEY6210, TN121, and TN124 backgrounds. In particular, SEY6210 and BY4741 or BY4742 contain large deletions in some of the alleles that prohibit homologous recombination with the corresponding wild-type alleles in most existing yeast plasmids.[21,22] This property severely limits the use of integration plasmids. Although it is still feasible to use centromeric plasmids, the transformants will always need to be maintained in selective media.

Approximately 2 decades ago, yeast genetic screenings conducted independently by several pioneering laboratories led to the discovery of the first batch of Atg proteins.[5] Their work ignited the explosion in modern autophagy research. Today, research in autophagy has expanded far beyond yeast. Nevertheless, yeast remains a major model system, in part owing to the wealth of tools and tricks available. The authors hope that the availability of this new tool set will ease the burden of routine microscopy work for our yeast colleagues and further accelerate yeast autophagy research.

Materials and Methods

Construction of plasmids and strains

For each C-terminal GFP tagging plasmid, yeast strain TN124 was first tagged with GFP to the corresponding Atg protein using the traditional PCR-based method.[6,7] The primers used for tagging are listed in **Table S4**. The genomic DNA of the resulting strain was used as a template to amply a fragment containing the C-terminal part of the ORF, the cassette inserted by the PCR method, and the region downstream (**Fig. S1**). The fragment was then inserted into Bluescript II SK+.[25] The primers and restriction enzyme used are listed in **Table S5**. For the 2xGFP set, we first introduced a second copy of GFP into KT209 (**Table S5**). Using this plasmid as a template, the whole set was constructed in the same way as the single GFP set.

For DRE-tagged Atg8, the ORF of DRE was cloned from PT4074–5 (Clontech, 632535).[16] The codons of the linker peptides were added by the cloning primers (**Table S5**). Four copies were inserted into Bluescript II SK+ to generate QuDre. It was subcloned into RS404,[26] and combined with promoter sequences and *ATG8* ORF to generate plasmids for the expression of chimeras in yeast (**Table S5**). Plasmid tdTomato-URA3-C1 was a gift from Dr. Anuj Kumar (University of Michigan, Ann Arbor). The promoter of *CUP1* and the ORF of *ATG8* were inserted into tdTomato-URA3-C1 to generate *CUP1*p-tdTomato-Atg8-URA3. Plasmids expressing *CUP1*p-mCherry-Atg8 and *ATG8*p-2xmCherry-Atg8 were gifts from Dr. Fulvio Reggiori (University of Groningen) and Dr. Kuninori Suzuki (University of Tokyo), respectively.[27,28] Both constructs were subcloned into RS404 before use.

Plasmids for the complementation of common auxotrophic markers (BS-His3, BS-Leu2, BS-Lys2, BS-Met15, BS-Trp1, BS-Ura3Kl) were designed so that they contain sufficient homologous regions for insertion into the genome even if large chunks of the corresponding marker genes were deleted. The primers and restriction enzyme used are listed in **Table S5**. In the case of *LYS2*, we used downstream sequence of *LEU2* as the insertion locus, because the *LYS2* gene was quite large and we were unable to get any longer fragments.

The plasmid for the single copy integration of *ATG8*p-GFP-Atg8 was constructed from BS-Ura3Kl. The *ATG8*p-GFP-Atg8 fragment was amplified from 1K-GFP-Atg8–406.[29] The resulting plasmid, BS-Ura3-GFP-Atg8, should be amplified by the following primers for single-copy integration: *BU3* F (5- CAG ACG ATG ATA ACA AAC CG -3), *BU3* R (5- GTT CGC TAT GCT TCA AGA AC -3).

Except for **Figure 3**, all strains used in the work were derived from TN124.[14]

Selection of linker sequences for tandem DRE constructs

The crystal structure of DRE protein was downloaded from the Protein Data Bank (PDB code 2V4E). Distances between chain 1 C terminus and chain 2 N terminus, chain 2 C terminus and chain 4 N terminus were found to be approximately 31 Å and 68 Å, respectively. We designated the linkers enlisted to connect these termini linker S and L, respectively (**Fig. S6**). A linker database (http://www.ibi.vu.nl/programs/linkerdbwww/) was searched for suitable candidates (**Tables S2, S3**).[17] The candidates were then joined to the termini using Modeler 9.10.[18] The conformations that penetrate through the β-barrel structure of DRE were discarded without further analysis. For the remaining ones, the most stable conformations were selected after energy minimization with Amber12.[19] Finally, root-mean-square deviations (RMSD) between the resulting tandem tetramers and the original DRE were calculated using BioLuminate 1.3 (SchrÖdinger, LLC, New York).

Fluorescence microscopy

Glass bottom 35 mm petridishes were coated with one mg/ml concanavalin A (Sigma-Aldrich, L7647). Prior to observation, yeast cells in liquid culture were allowed to sediment on the coated glass surface for about 5 to 10 mins. The dishes were gently washed, and fresh liquid media were added. The samples were then examined in an Olympus IX81 microscope (Olympus Corporation, Tokyo, Japan) equipped with an Andor DV885 camera (Andor Technology Ltd, Belfast, UK), or an Olympus IX83 microscope (Olympus Corporation, Tokyo, Japan) equipped with a Hamamatsu ORCA-Flash4.0 LT camera (Hamamatsu Photonics K.K., Hamamatsu City, Japan). For each sample, a Z-stack of 15 images was collected, with 0.5 μm stepping. After visual inspection, 10 consecutive sections that cover the entire depth of yeast cells were chosen to create a max-intensity projection.

Other methods

Culturing of yeast cells, Ape1 western blotting, and the Pho8Δ60 assay were performed as previously described.[13,14,30]

Disclosure of Potential Conflicts of Interest

No potential conflicts of interest were disclosed.

Acknowledgments

The authors would like to thank Drs. Daniel J. Klionsky (University of Michigan, Ann Arbor), Anuj Kumar (University of Michigan, Ann Arbor), Gary D. Luker (University of Michigan, Ann Arbor), Yoshinori Ohsumi (Tokyo Institute of Technology), Fulvio Reggiori (University of Groningen) and Kuninori Suzuki (University of Tokyo) for gifts of plasmids and reagents, and thank Dr. Li Yu (Tsinghua University) and Ms. Ying-Fei Zhu (Nankai University) for technical assistance.

Funding

This work was supported by National Natural Science Foundation of China grants 31471301, 31222034 and 31171285, and National Key Basic Research Program of China grant 2011CB910100 to Z. X.

Supplemental Material

Supplemental data for this article can be accessed on the publisher's website

References

1. Xie Z, Klionsky DJ. Autophagosome formation: core machinery and adaptations. Nat Cell Biol 2007; 9:1102-9; PMID:17909521; http://dx.doi.org/10.1038/ncb1007-1102

2. Nakatogawa H, Suzuki K, Kamada Y, Ohsumi Y. Dynamics and diversity in autophagy mechanisms: lessons from yeast. Nat Rev Mol Cell Biol 2009; 10:458-67; PMID:19491929; http://dx.doi.org/10.1038/nrm2708
3. Mizushima N, Yoshimori T, Ohsumi Y. The role of Atg proteins in autophagosome formation. Ann Rev Cell Dev Biol 2011; 27:107-32; PMID:21801009; http://dx.doi.org/10.1146/annurev-cellbio-092910-154005
4. Reggiori F, Klionsky DJ. Autophagic processes in yeast: mechanism, machinery and regulation. Genetics 2013; 194:341-61; PMID:23733851; http://dx.doi.org/10.1534/genetics.112.149013
5. Klionsky DJ, Cregg JM, Dunn WA Jr, Emr SD, Sakai Y, Sandoval IV, Sibirny A, Subramani S, Thumm M, Veenhuis M, et al. A unified nomenclature for yeast autophagy-related genes. Dev Cell 2003; 5:539-45; PMID:14536056; http://dx.doi.org/10.1016/S1534-5807(03)00296-X
6. Longtine MS, McKenzie A 3rd, Demarini DJ, Shah NG, Wach A, Brachat A, Philippsen P, Pringle JR. Additional modules for versatile and economical PCR-based gene deletion and modification in Saccharomyces cerevisiae. Yeast 1998; 14:953-61; PMID:9717241; http://dx.doi.org/10.1002/(SICI)1097-0061(199807)14:10%3c953::AID-YEA293%3e3.0.CO;2-U
7. Sheff MA, Thorn KS. Optimized cassettes for fluorescent protein tagging in Saccharomyces cerevisiae. Yeast 2004; 21:661-70; PMID:15197731; http://dx.doi.org/10.1002/yea.1130
8. Suzuki K, Kirisako T, Kamada Y, Mizushima N, Noda T, Ohsumi Y. The pre-autophagosomal structure organized by concerted functions of APG genes is essential for autophagosome formation. EMBO J 2001; 20:5971-81; PMID:11689437; http://dx.doi.org/10.1093/emboj/20.21.5971
9. Kim J, Huang WP, Stromhaug PE, Klionsky DJ. Convergence of multiple autophagy and cytoplasm to vacuole targeting components to a perivacuolar membrane compartment prior to de novo vesicle formation. J Biol Chem 2002; 277:763-73; PMID:11675395; http://dx.doi.org/10.1074/jbc.M109134200
10. Shaner NC, Patterson GH, Davidson MW. Advances in fluorescent protein technology. J Cell Sci 2007; 120:4247-60; PMID:18057027; http://dx.doi.org/10.1242/jcs.005801
11. Shcherbakova DM, Subach OM, Verkhusha VV. Red fluorescent proteins: advanced imaging applications and future design. Angewandte Chemie 2012; 51:10724-38; PMID:22851529; http://dx.doi.org/10.1002/anie.201200408
12. Mizushima N, Noda T, Yoshimori T, Tanaka Y, Ishii T, George MD, Klionsky DJ, Ohsumi M, Ohsumi Y. A protein conjugation system essential for autophagy. Nature 1998; 395:395-8; PMID:9759731; http://dx.doi.org/10.1038/26506
13. Klionsky DJ, Cueva R, Yaver DS. Aminopeptidase I of Saccharomyces cerevisiae is localized to the vacuole